2009 American Control Conference
Hyatt Regency Riverfront, St. Louis, MO, USA
June 10-12, 2009

Near Real-Time System Identification in a Wireless Sensor Network for Adaptive Feedback Control

R. Andrew Swartz, Jerome P. Lynch, *Member, IEEE*, and Chin-Hsiung Loh, *Member, IEEE*

Abstract—**Migration of the identified system poles for a dynamical system indicates changes in its global properties. In civil engineering structures, these changes are most often due to changes in global stiffness or damping parameters associated with both environmental effects as well as deterioration of the structure. In structures that employ automated feedback control systems to mitigate unwanted vibrations, feedback control laws and state estimators (if used) are reliant upon a theoretical or identified model of the plant. Any loss in fidelity between the plant model and its actual condition will result in degradation of the controller performance. Low-cost, wireless control networks that by nature are more likely to utilize state-estimation, are therefore more vulnerable to problems associated with property changes in the system. In this paper, recursive identification of system poles is proposed for use in a wireless sensing network engaged in feedback control. Because it is based on system poles, the algorithm is ideally suited for adaptive control methods that update control and estimation gains as system properties change. The algorithm proposed is based on the fast transversal filter and is designed to minimize computation as well as data transmission requirements to optimally utilize the distributed data that is stored within a low-power wireless sensor network.**

I. Introduction

FEEDBACK control is gaining popularity in civil engineering applications for mitigation of undesirable mechanical vibrations induced by natural sources, such as wind and seismic loads, as well as artificial sources, such as mechanical equipment [1-3]. Such systems enhance the safety and comfort level of occupants and may also aid in the proper operation of sensitive equipment housed within the structure. In civil engineering control applications, economy and reliability are especially critical. Semi-active actuators that indirectly generate control forces (e.g. variable-orifice dampers, magnetorheological dampers, *etc*.) are one solution for addressing the cost and reliability concerns associated with active control technologies. Significantly less expensive than large, centralized actuators, semi-active actuators may be installed in large numbers (in the hundreds) reducing the susceptibility of the control system to single-points of failure [4-6]. In coordinated control networks though, a large number of actuators will require extensive cabling to connect the actuators to the sensing and control computation portions of the network. Such cabling can quickly erode the cost savings benefits realized from use of semi-active dampers [7]. Wireless networks may be used to eliminate the costs associated with cables (thousands of dollars per channel [8]) but come with their own challenges, namely battery power limitations and spatially distributed data. Limiting the amount of data transmitted between nodes of the wireless network, is important to conserve battery power. Instead, leveraging the local computing power of the wireless node to reduce transmissions will conserve power [9]. In control applications, spatially distributed data may be estimated locally to decrease dependence upon limited wireless bandwidth [7, 10].

As with any feedback control system, proper operation is dependent upon good design, based on knowledge of the dynamic characteristics of the plant. In systems reliant on state estimation, this fact is especially true. Over the years many techniques have been developed to ensure robust controller performance in the face of uncertain, or incompletely characterized plant models. More difficult still are cases in which the plant dynamics change over time in which, depending upon the degree of the changes, adaptive control methods may become necessary.

In civil structural systems, changes in the global vibrational characteristics are inevitable over time. In the short term, environmental factors such as temperature and humidity have a significant influence upon the stiffness of civil structures affecting the location of the poles of the plant. Longer term effects such as damage due to overstress, fatigue, or loss of connectivity between components (e.g. loss of tension in bolts) will also lead to changes in the plant. Even effects that are considered normal for civil structures (and are accounted for in design) such as cracking in concrete within its design operational range and creep effects (particularly in concrete and wood structures) while not qualifying as damage, *per se*, do change the vibrational characteristics of the structure and will adversely affect feedback control performance.

In this paper, a plant model updating method is proposed for adaptive control applications in civil structures using low-cost wireless control networks. The method is based on Structural Health Monitoring (SHM) methods for correlating changes in dynamic properties of the system to damage. The method presented utilizes spatially distributed acceleration data to calculate and recursively update system poles of a

Manuscript received September 14, 2008. This work was supported in part by the NSF under Grant CMMI-0726812.

R. A. Swartz is with the Department of Civil and Environmental Engineering, University of Michigan, Ann Arbor, MI 48109 USA (e-mail: asgard@ umich.edu).

J. P. Lynch is with the Department of Civil and Environmental Engineering, University of Michigan, Ann Arbor, MI 48109 USA (phone: 734-615-5290; fax: 734-764-4292; e-mail: jerlynch@umich.edu).

C.-H. Loh is with the Department of Civil Engineering, National Taiwan University, Taipei, Taiwan, (e-mail: lohc0220@ntu.edu.tw).

civil structure. The method is based on auto-regressive with exogenous inputs (ARX) models calculated by the fast transversal filter (FTF), a computationally efficient recursive least-squares filter well suited to use in low-power wireless networks. Results of the FTF are used to assemble the discrete-time transfer function corresponding to a given output. The roots of the characteristic equation represent the poles of the system. These roots are calculated from the QR-decomposition of the polynomial's companion matrix. Tracking the migration of system poles is well suited for updating state-space control algorithms that are based on optimal placement of poles on the complex z-plane. The method is demonstrated on a six-story shear structure with removable bracing elements that are gradually weakened to simulate damage. Results are presented in the form of system pole migration and quantified in terms of three damage indices that track the extent of change.

II. THEORY AND BACKGROUND

Of the wide array of models available for modeling the relationship between inputs and outputs in linear time-invarient (LTI) systems, one that is simple and useful is the linear difference equation. The discrete-time model consists of m and n weighted observations of the output, $y[k]$, and input, $u[k]$, respectively:

$$\begin{aligned} y[k] + a_1 y[k-1] + \cdots + a_m y[k-m] \\ = b_0 u[k] + b_1 u[k-1] + \cdots \\ + b_n u[k-n] + e[k] \end{aligned} \tag{1}$$

where $e[k]$ is the error at the kth time step, a and b are the observation weights and, for models not including a direct transmission term, $b_0 = 0$. One can rearrange the difference equation to form an estimate of the kth output based on the weighted past observations [11]:

$$\begin{aligned} \hat{y}[k] = -a_1 y[k-1] - \cdots - a_m y[k-m] + b_0 u[k] \\ + b_1 u[k-1] + \cdots + b_n u[k-n] \end{aligned} \tag{2}$$

This equation represents the auto-regressive with exogenous inputs (ARX) time-series model. The difference equation is transformed into a transfer equation through means of the Z-transform:

$$F(z) = \sum_{k=-\infty}^{\infty} f[k] z^{-k} \tag{3}$$

the discrete-time analog of the Laplace transform. In the z-domain, the ARX derived transfer function relating an input to an output takes the familiar form (setting the number or input and output observations to p):

$$H(z) = \frac{Y(z)}{U(z)} = \frac{b_0 z + b_1 z^{-1} + \cdots + b_p z^{-p}}{1 + a_1 z^{-1} + \cdots + a_p z^{-p}} \tag{4}$$

The denominator of (4) is the characteristic equation whose roots are the poles of the system. These poles encapsulate the modal properties of the system including modal frequencies and damping ratios. The numerator of the transfer function is also a polynomial function whose roots are the zeros of the system.

To determine the ARX model weighting coefficients (a and b), typically linear least-squares methods are used. For example, if large amounts of memory and computational throughput are available, a batch least-squares solution will be adequate. However, if one desires to implement the batch least-squares methods in resource-constrained computing environments (e.g. wireless sensors) real-time or near real-time execution would likely not be possible. An alternative approach to ARX model determination would be through the use of recursive methods such as the fast transversal filter (FTF).

In this study, the FTF is employed for embedment in wireless sensors because it represents a significant reduction in computational overhead compared to many of the other recursive least-squares algorithms available. In the FTF, the number of computations needed and required memory increase linearly with the model order, O(p), unlike classical recursive least-squares which increase by the square of the model order, O(p^2) [12]. In low-power wireless sensor applications, these computational savings are necessary to compute the transfer function with reasonable speed. The FTF takes advantage of the shifting property, including a forward-time and backward-time output estimator. The coefficients of the forward-time estimator are the ARX coefficients that define the transfer function to be identified. The FTF employs the *a priori* and *a posteriori* errors in the backward and forward time estimators to update the estimators and the estimator update gains. A complete derivation of the FTF may be found in [13] or [14]. A description of the FTF derived for a single-input single-output (SISO) system with a direct transmission term is given by Juang [12] and presented in Table 1. The FTF may be initialized from theoretical values, assuming zero initial conditions [14], or based on an offline batch FTF solution using pre-recorded data [12]. In this study, the latter approach is utilized, employing a forgetting factor, λ, multiplying the old error squares terms in (9) and (21) to de-emphasize older observations so that new trends will become apparent.

While the FTF can be executed faster than the recursive least-squares algorithm, it does suffer from instabilities when implemented on a finite precision computer. Unstable modes exist within the filter that are not excited by infinite precision arithmetic. In real systems with finite precision, the stability of the filter is dependent upon both the degree of precision of the processor as well as the characteristics of the

Table 1. Summary of FTF Algorithm

Forward-time Estimation		
data history vector, $v_p[k\text{-}1]$	$\boldsymbol{v_p}[k-1] = \begin{bmatrix} u[k] \\ y[k-1] \\ u[k-1] \\ \vdots \\ y[k-p] \\ u[k-p] \end{bmatrix}$	(5)
new data vector, $\boldsymbol{y_{\vec{u}}}[k]$	$\boldsymbol{y_{\vec{u}}}[k] = \begin{bmatrix} u[k+1] \\ y[k] \end{bmatrix}$	(6)
a priori error, $\vec{\boldsymbol{e}}_p^-[k]$	$\vec{\boldsymbol{e}}_p^-[k] = \boldsymbol{y_{\vec{u}}}[k] - \hat{\vec{\boldsymbol{Y}}}_p[k-1]\boldsymbol{v_p}[k-1]$	(7)
a posteriori error, $\vec{\boldsymbol{e}}_p^+[k]$	$\vec{\boldsymbol{e}}_p^+[k] = \gamma_p[k-1]\,\vec{\boldsymbol{e}}_p^-[\boldsymbol{k}]$	(8)
error squares, $\vec{\boldsymbol{\varepsilon}}_p[k]$	$\vec{\boldsymbol{\varepsilon}}_p[k] = \vec{\boldsymbol{\varepsilon}}_p[k-1] + \vec{\boldsymbol{e}}_p^+[\vec{\boldsymbol{e}}_p^-]^{\mathrm{T}}$	(9)
observation weights, $\hat{\vec{\boldsymbol{Y}}}_p[k]$	$\hat{\vec{\boldsymbol{Y}}}_p[k] = \hat{\vec{\boldsymbol{Y}}}_p[k-1] + \vec{\boldsymbol{e}}_p^-[k]\boldsymbol{G_p}[k-1]$	(10)
augmented gain, $G_{p+1}[k]$	$G_{p+1}[k] = \left[\left[\vec{\boldsymbol{e}}_p^+[k]\right]^{\mathrm{T}}\vec{\boldsymbol{\varepsilon}}_p^{-1}[k] \quad \boldsymbol{G_p}[k-1] - [\vec{\boldsymbol{e}}_p^+[k]]^{\mathrm{T}}\vec{\boldsymbol{\varepsilon}}_p^{-1}[k]\hat{\vec{\boldsymbol{Y}}}_p[k]\right]$	(11)
augmented conversion factor, $\gamma_{p+1}[k]$	$\gamma_{p+1}[k] = \gamma_p[k-1] - [\vec{\boldsymbol{e}}_p^+[k]]^{\mathrm{T}}\vec{\boldsymbol{\varepsilon}}_p^{-1}[k]\vec{\boldsymbol{e}}_p^+[k]$	(12)
decompose augmented gain	$\boldsymbol{G_{p+1}}[k] = \left[\boldsymbol{G}_{p+1}^{(r)}[k] \quad \boldsymbol{G}_{p+1}^{(a)}[k]\right]$	(13)
Backward-time Estimation		
data history vector, $v_p[k]$	$\boldsymbol{v_p}[k] = \begin{bmatrix} u[k+1] \\ y[k] \\ u[k] \\ \vdots \\ y[k-p+1] \\ u[k-p+1] \end{bmatrix}$	(14)
data vector, $\boldsymbol{y_u}[k-p]$	$\boldsymbol{y_u}[k-p] = \begin{bmatrix} y[k+p] \\ u[k-p] \end{bmatrix}$	(15)
a priori error, $\overleftarrow{\boldsymbol{e}}_p^-[k]$	$\overleftarrow{\boldsymbol{e}}_p^-[k] = \boldsymbol{y_u}[k-p] - \hat{\overleftarrow{\boldsymbol{Y}}}_p[k-1]\boldsymbol{v_p}[k]$	(16)
gain, $\boldsymbol{G_p}[k]$	$\boldsymbol{G_p}[k] = \dfrac{\boldsymbol{G}_{p+1}^{(r)}[k] + \boldsymbol{G}_{p+1}^{(a)}[k]\hat{\overleftarrow{\boldsymbol{Y}}}_p[k-1]}{1 - \boldsymbol{G}_{p+1}^{(a)}[k]\overleftarrow{\boldsymbol{e}}_p^-[k]}$	(17)
observation weights, $\hat{\overleftarrow{\boldsymbol{Y}}}_p[k]$	$\hat{\overleftarrow{\boldsymbol{Y}}}_p[k] = \hat{\overleftarrow{\boldsymbol{Y}}}_p[k-1] + \overleftarrow{\boldsymbol{e}}_p^-[k]\boldsymbol{G_p}[k]$	(18)
conversion factor, $\gamma_p[k]$	$\gamma_p[k] = \dfrac{\gamma_{p+1}[k]}{1 - \boldsymbol{G}_{p+1}^{(a)}[k]\overleftarrow{\boldsymbol{e}}_p^-[k]}$	(19)
a posteriori error, $\overleftarrow{\boldsymbol{e}}_p^+[k]$	$\overleftarrow{\boldsymbol{e}}_p^+[k] = \gamma_p[k]\overleftarrow{\boldsymbol{e}}_p^-[k]$	(20)
error squares, $\overleftarrow{\boldsymbol{\varepsilon}}_p[k]$	$\overleftarrow{\boldsymbol{\varepsilon}}_p[k] = \overleftarrow{\boldsymbol{\varepsilon}}_p[k] + \overleftarrow{\boldsymbol{e}}_p^+[k][\overleftarrow{\boldsymbol{e}}_p^-[k]]^{\mathrm{T}}$	(21)

excitation signals [15, 16]. This effect is exacerbated if a forgetting factor is used [17]. Slock and Kailath [15] present a stabilization solution for the FTF taking advantage of

Fig. 1. Six-story test structure.

quantities in the FTF algorithm that are computed using both the forward-time and backward-time estimator. In infinite precision systems these quantities will be calculated to be the same for both estimators. As precision errors are introduced, there exists an error between the forward-time and backward-time calculations. Slock and Kailath essentially use these errors as feedback signals to stabilize the FTF filter. A simpler method presented by Binde [17] will be used in this paper. In this second method, "leakage correction factors" that are less than, but nearly equal to 1 are introduced into the filter equations (10) and (18) to control the propagation of errors. Soh and Douglas [18] confirm the effectiveness of the leakage correction method for real-world signals and forgetting factors (λ) that are nearly 1.

In this study, the FTF is implemented on a finite precision microcontroller (fixed-point, 8-bit) with a leakage factor included to ensure stability of the filter. Data is then collected and run through the FTF algorithm updating the forward-time estimation weighting factors. Those weighting factors corresponding to the characteristic equation are then assembled to form its companion matrix. A QR-decomposition algorithm [19] is then run on the companion matrix to find its eigenvalues which are the roots of the characteristic equation and thus, system poles. This method works well when eigenvalues are not repeated, otherwise it will run into numerical problems.

III. Narada Wireless Sensor

The wireless sensing platform employed in this study is based on the *Narada* wireless sensor developed at the University of Michigan [20]. The sensor is designed around

Table 2. Damage case bracing element schedule.

FLOOR	B_I	1	2	B_{II}	3	4	5
6F	B3	B3	B3	B3	B3	B3	B3
5F	B3	B3	B3	B3	B3	B3	B3
4F	B3	B3	B3	B3	B3	B3	B3
3F	B3	B3	B3	B3	B3	B2	B3
2F	B3	B3	B3	B3	B2	B1	B3
1F	B3	B2	B1	B3	B1	Removed	B4

Table 3. Bracing description.

	Length (cm)	Width (cm)	Thickness (cm)
Columns	95	15	2.5
Brace B1	21	3	1
Brace B2	21	5	1
Brace B3	21	10	1
Brace B4	10	3	0.5

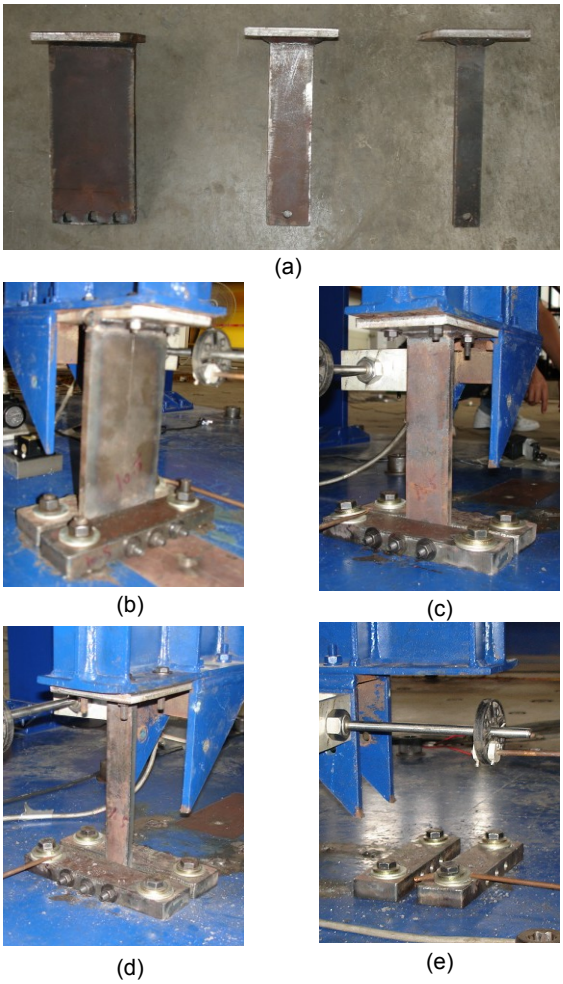

Fig. 2. Bracing elements, (a)left to right, B3, B2, and B1, (b) B3 installed, (c) B2 installed, (d) B1 installed, (e) braces removed.

a computational core including the 8-bit Atmel Atmega128 microcontroller. It has 128k of flash memory, 4k of SRAM, and an additional 128k of external SRAM for data storage is included in the sensor design. The sensing interface consists of a 4-channel, 16-bit Texas Instruments (TI) ADS8341 analog to digital converter (ADC). The communications interface consists of a TI CC2420 2.4 GHz spread spectrum radio that conforms to the IEEE 802.15.4 protocol. To participate in control networks, the sensor also includes a 2-channel, 12-bit TI DAC7612 digital to analog converter (DAC) as an actuation interface.

A library of embedded algorithms has been developed for the *Narada* wireless sensor for a number of applications. Data collection algorithms are at the core of its operation, but additional algorithms including FFT, wavelet transform, singular value decomposition, eigenvalue and eigenvector solver, static Kalman estimation, state-feedback control, peak picking, frequency-domain decomposition, random decrement, batch least squares, classical recursive least squares, and FTF have been developed for structural health monitoring, modal analysis, and feedback control applications. This study will specifically leverage the data collection, FTF, and eigenvalue solver algorithms to identify and update system poles of the structure being monitored.

IV. Experimental Setup

The test structure that is the subject of this study is a six-story, one-third scale, steel building located at the National Center for Research in Earthquake Engineering (NCREE) at National Taiwan University (NTU). The structure has a floor-to-floor height of 1.0 m, width of 1.0 m, and depth of 1.5 m. Floors are 2.0 cm thick plates supported on four sides by 5 cm x 5 cm L-sections. The L-sections are bolted to 2.5 cm x 15 cm bar columns that run continuously the entire height of the structure (Fig. 1). To simulate damage, first the structure is stiffened using very stiff chevron bracing between adjacent floors. At the bottom of each brace, stiffness elements consisting of 1.0 cm x 10.5 cm plates, loaded in their weak direction are connected between the bracing and the floor below. This stiffened structure is considered to be the baseline, or initial, undamaged structure, that the control models are to be based upon. Damage is then introduced by replacing original stiffness elements with weaker elements to simulate reduced story stiffness due to damage. Table 2 tabulates which braces are used in each damage case (case 1 through 5), Fig. 2 depicts the weak bracing elements, while Table 3 summarizes the size of the brace elements used.

The structure is placed on a 5 m x 5 m, 6 degree of freedom (DOF) shaking table to simulate earthquake excitation. The structure is then instrumented with a network of 19 *Narada* wireless sensors with accelerometers attached, two on each floor measuring acceleration in the structure's weak lateral direction, one on each floor measuring acceleration in the structure's strong lateral direction, and one at the base measuring lateral ground motion. The base unit is configured to broadcast ground

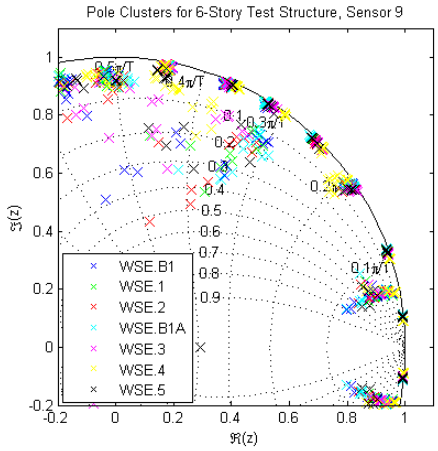

Fig. 3. Identified poles in the upper right quadrant of the unit circle for baseline (B_I and B_{II}) and damage cases 1-5.

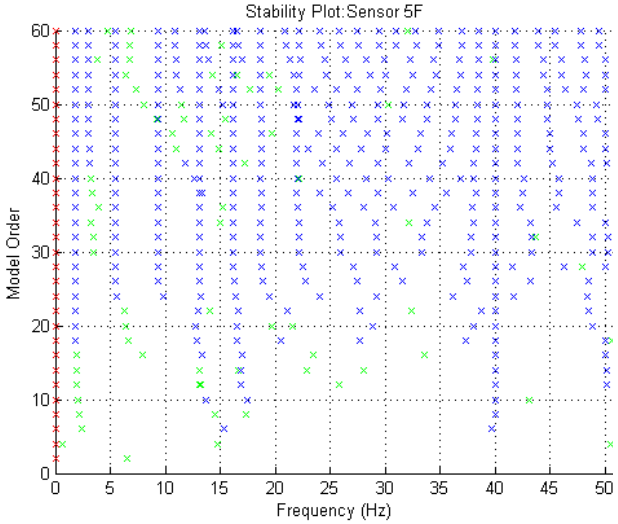

Fig. 4. Stability diagram generated by the 5th floor, front sensor.

motion measurements to the rest of the network to be used as the input signal and, as such, is supplied with a permanent power supply whereas the remote units rely on battery packs for power. A tethered data acquisition system is also installed on the structure for comparison to the wireless system results. Operation of the wireless system was done through a laptop computer with its own CC2420 transmitter. Test runs consist of unidirectional (lateral weak direction) and bidirectional (both lateral directions) broad spectrum excitations of the structure using the shaking table. Migration of the system poles is measured through use of a migration index adapted from Swartz and Lynch [21]:

$$SI_{distance} = \frac{\Delta_i}{\sigma_i} \tag{24}$$

V. Results

An ARX model with equal numbers of inputs and outputs and a direct transmission term is constructed for the six-story test structure. A model order of p=36 is required to cause the lower frequency poles to converge to the theoretical values. Then the poles corresponding to the lowest set of six resonant frequencies are selected for migration tracking as these are the poles that would be used in a state-space model for feedback control. The remaining poles are ignored. Due to environmental variability and sensor noise, repeated identifications of the system poles will yield small variations in pole locations independent of damage. The result is that multiple identification runs will produce roughly Gaussian "clusters" of poles around their true locations. Pole clusters of 8 to 14 poles per damage case are calculated (some by cabled data to fill out the data set despite limited availability of shaking table time). Those pole clusters corresponding to the damage cases of Table 2 are plotted in Fig. 3. Zoomed in views of pole cluster 2 for the twelve weak direction sensors are plotted in Fig. 5 to show pole cluster migration. Greater losses in stiffness yield greater pole migration. For the revisited baseline case, the pole clusters revert back to their original location.

In order to combine the damage indices that quantify the degree of pole migration as well as decide on updated system poles to use for control, the network must decide which results are most trustworthy by examining the expected signal-to-noise ratio (requires mode shapes). Lack of adequate excitation of a given mode at a given sensor will produce pole migration results that may not correspond to the true changes in the behavior of the system. Operational deflection shapes based on broad-band, white excitation are computed from the imaginary portion of the frequency response functions at the resonant frequencies. A damage index based on the normalized separation distance between the centers of the identified test pole clusters versus the baseline pole clusters has been developed. The resulting damage cases (along with their average) are presented in Fig. 6. The separation index also indicates the greater degree of pole separation as the properties of the system change.

VI. Conclusion

In this paper a method for updating plant models for feedback control in civil structures is presented. The method is computationally efficient and requires minimal transmission of data between spatially separated data repositories, such as is the case in wireless networks. A separation index developed to track these changes may then be used to indicate the severity of the changes in the underlying plant. The updated plant models can be then leveraged to update control gains using pole placing techniques and improve controller performance.

The time required to compute an updated system model on the embedded system is highly dependent upon both model size and model structure both due to the relatively

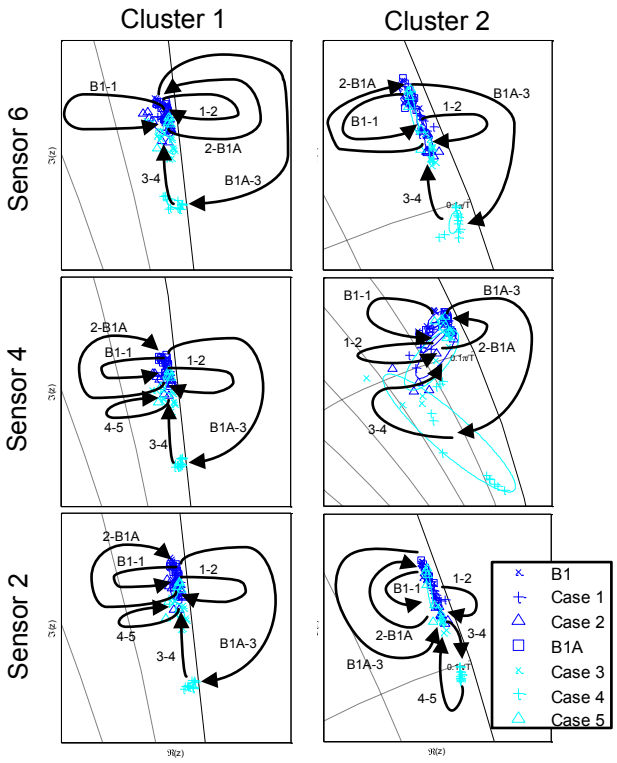

Fig. 5. Pole cluster migration by damage case for the first two modal frequencies.

high computational overhead inherent in this sort of power-constrained system and the more stringent bandwidth limitation inherent in wireless networking. For the model sizes and architecture used in this study, the algorithm runs at approximately 15 Hz, meaning that it will run behind real-time applications, updating the model periodically rather than continuously. The advantage of this approach over more network-centric system identification approaches (*e.g.* the Eigenvalue Realization Algorithm or Subspace Identification) is that it produces a reasonable solution while minimizing the amount of raw data transmission, which incurs not only significant additional (and non-deterministic) latency, but quickly exhausts battery power through radio usage. As with any engineering algorithm, speed, accuracy, cost, and power requirements must be carefully considered.

REFERENCES

[1] G. W. Housner, L. A. Bergman, T. K. Caughey, A. G. Chassiakos, R. O. Claus, S. F. Masri, R. E. Skelton, T. T. Soong, B. F. Spencer Jr., and J. T. P. Yao, "Structural control: past, present, and future," *Journal of Engineering Mechanics*, vol. 123, pp. 897-971, 1997.

[2] T. T. Soong, *Active Structural Control: Theory and Practice*. Essex, England: Longman Scientific and Technical, 1990.

[3] B. F. Spencer and S. Nagarajaiah, "State of the art of structural control," *Journal of Structural Engineering*, vol. 129, pp. 845-856, 2003.

[4] N. Kurata, T. Kobori, M. Takahashi, N. Niwa, and H. Midorikawa, "Actual seismic response controlled building with semi-active damper system," *Earthquake Engineering and Structural Dynamics*, vol. 28, pp. 1427-1447, 1999.

[5] P.-Y. Lin, P. N. Roschke, and C.-H. Loh, "System identification and real application of a smart magneto-rheological damper," presented at 2005 International Symposium on Intelligent Control, Limassol, Cyprus, 2005.

[6] S. J. Dyke, B. F. Spencer Jr., and M. K. Sain, "An experimental study of MR dampers for seismic protection," *Smart Materials and Structures*, vol. 7, pp. 693-703, 1998.

[7] R. A. Swartz and J. P. Lynch, "Strategic Utilization of Limited Bandwidth in a Wireless Control System for Seismically Excited Civil Structures," *Jornal of Structural Engineering*, In Press.

[8] M. Celebi, "Seismic Instrumentation of Buildings (with emphasis on federal buildings)," United States Geologic Survey (USGS), Menlo Park, CA, U.S.A. 0-7460-68170, 2002.

[9] E. Straser and A. S. Kiremidjian, "Modular, Wireless Damage Monitoring System for Structures," John A. Blume Earthquake Engineering Center, Stanford, CA 128, 1998.

[10] Y. Wang, R. A. Swartz, J. P. Lynch, K. H. Law, K.-C. Lu, and C.-H. Loh, "Decentralized civil structural control using real-time wireless sensing and embedded computing," *Smart Structures and Systems*, vol. 3, pp. 321-340, 2007.

[11] L. Ljung, *System Identification, Theory for the User*, 2nd ed. Upper Saddle River, NJ: Prentice Hall, 1999.

[12] J.-N. Juang, *Applied System Identification*. Upper Saddle River, NJ: Prentice Hall, 1994.

[13] J. M. Cioffi and T. Kailath, "Fast, Recursive-Least-Squares Transversal Filters for Adaptive Filtering," *IEEE Transactions on Accoustics, Speech, and Signal Processing*, vol. ASSP-32, pp. 304-337, 1984.

[14] S. Haykin, *Adaptive Filter Theory*, 2nd ed. Englewood Clifs, NJ: Prentice Hall, 1991.

[15] D. T. M. Slock and T. Kailath, "Numerically Stable Fast Transversal Filters for Recursive Least Squares Adaptive Filtering," *IEEE Transactions on Signal Processing*, vol. 39, pp. 92-114, 1991.

[16] S. Haykin, *Adaptive Filter Theory*, vol. 3rd. Upper Saddle River, NJ: Prentice Hall, 1996.

[17] S. Binde, "A Numerically Stable Fast Transversal Filter with Leakage Correction," *IEEE Signal Processing Letters*, vol. 2, pp. 114-116, 1995.

[18] J. K. Soh and S. C. Douglas, "Analysis of the stabilized FTF Algorithm with Leakage Correction," presented at 1996 30th Asilomar Conference on Signals, Systems & Computers, Pacific Grove, CA, USA, 1997.

[19] W. H. Press, B. P. Flannery, S. A. Teukolsky, and W. T. Vetterling, *Numerical Recipes in C: The Art of Scientific Computing*, 2nd ed. Cambridge, U.K.: Cambridge University Press, 1992.

[20] A. Swartz, D. Jung, J. P. Lynch, Y. Wang, D. Shi, and M. P. Flynn, "Design of a wireless sensor for scalable distributed in-network computation in a structural health monitoring system," presented at 5th International Workshop on Structural Health Monitoring, Stanford, CA, 2005.

[21] R. A. Swartz and J. P. Lynch, "Damage Characterization of the Z24 Bridge by Transfer Function Pole Migration," presented at Proceedings of the 26th International Modal Analysis Conference (IMAC XXVI), Orlando, FL, U.S.A., 2008.

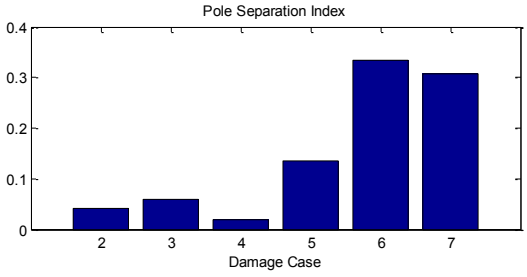

Fig. 6. Separation index results by damage case.